Statistical Wind-Tunnel Experimentation Advancements for eVTOL Aircraft Aero-Propulsive Model Development

Benjamin M. Simmons and Ronald C. Busan
Flight Dynamics Branch
NASA Langley Research Center

AIAA SciTech Forum
08–12 January 2024

Contents

- Research motivation
- RAVEN background
- Static wind-tunnel testing
  - Gravitational tare modeling
  - Trim envelope determination
  - Powered-airframe characterization
- Concluding remarks
- Questions/discussion

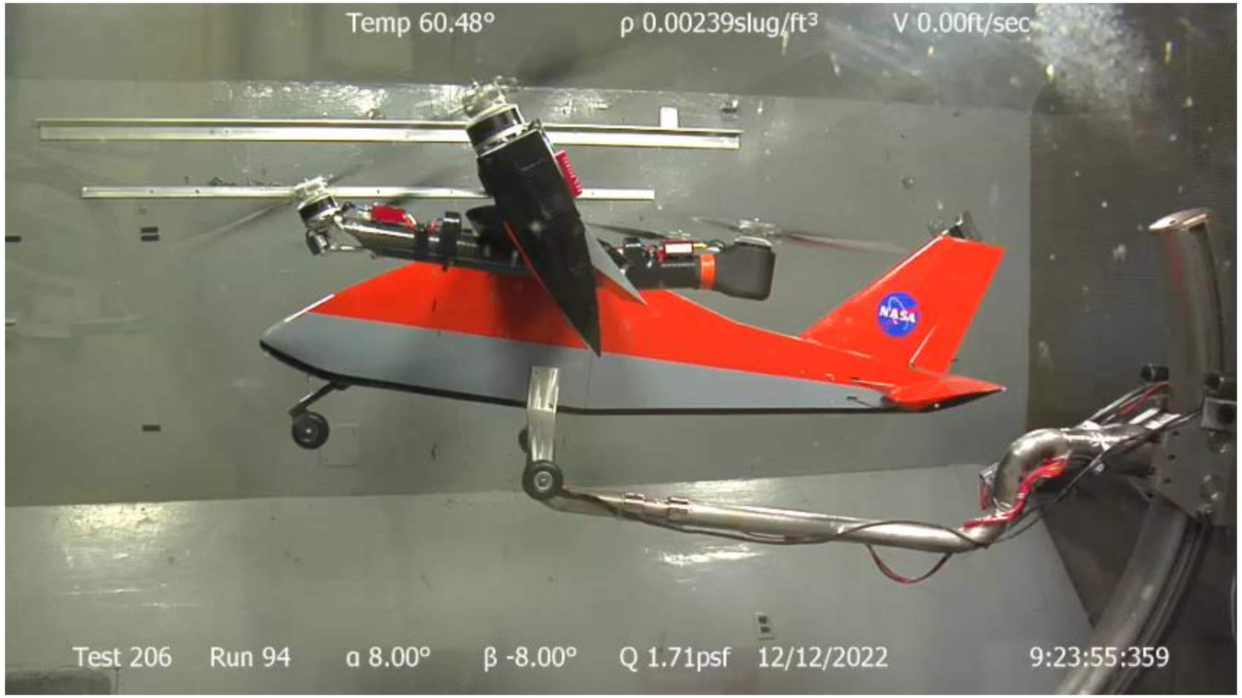

NASA RAVEN-SWFT wind-tunnel testing.

Software:
- Design-Expert®
- SIDPAC

Research Motivation

- Distributed propulsion aircraft enabling Advanced Air Mobility (AAM) missions
  - VTOL, STOL, and CTOL configurations
  - Many control surfaces and propulsors
  - Significant propulsion-airframe interactions
- Conventional methods fail to efficiently characterize complex aircraft
- Design of experiments (DOE) and response surface methodology (RSM) are essential
- Advance DOE/RSM strategies for characterization of complex aircraft
- Aero-propulsive modeling for a new electric vertical takeoff and landing (eVTOL) aircraft

NASA GL-10 aircraft

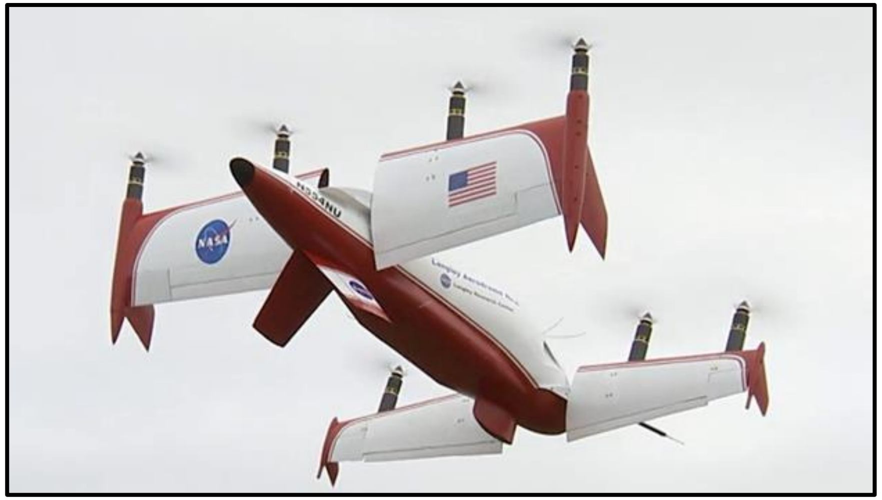

NASA LA-8 aircraft

RAVEN eVTOL Vehicle

- RAVEN – **R**esearch **A**ircraft for e**V**TOL **E**nabling Tech**N**ologies[1]
- Tilt-rotor eVTOL configuration with six variable-pitch proprotors
- Vehicles at different scales
- 24 independent control effectors
  - Six proprotor speeds ($n_1, n_2, \ldots, n_6$)
  - Six collective angles ($\delta_{c_1}, \delta_{c_2}, \ldots, \delta_{c_6}$)
  - Four nacelle tilt angles ($\delta_{t_1}, \delta_{t_2}, \delta_{t_3}, \delta_{t_4}$)
  - Six flaperons ($\delta_{f_1}, \delta_{f_2}, \ldots \delta_{f_6}$)
  - Stabilator (δ_s)
  - Rudder (δ_r)
- Built for modeling/controls research

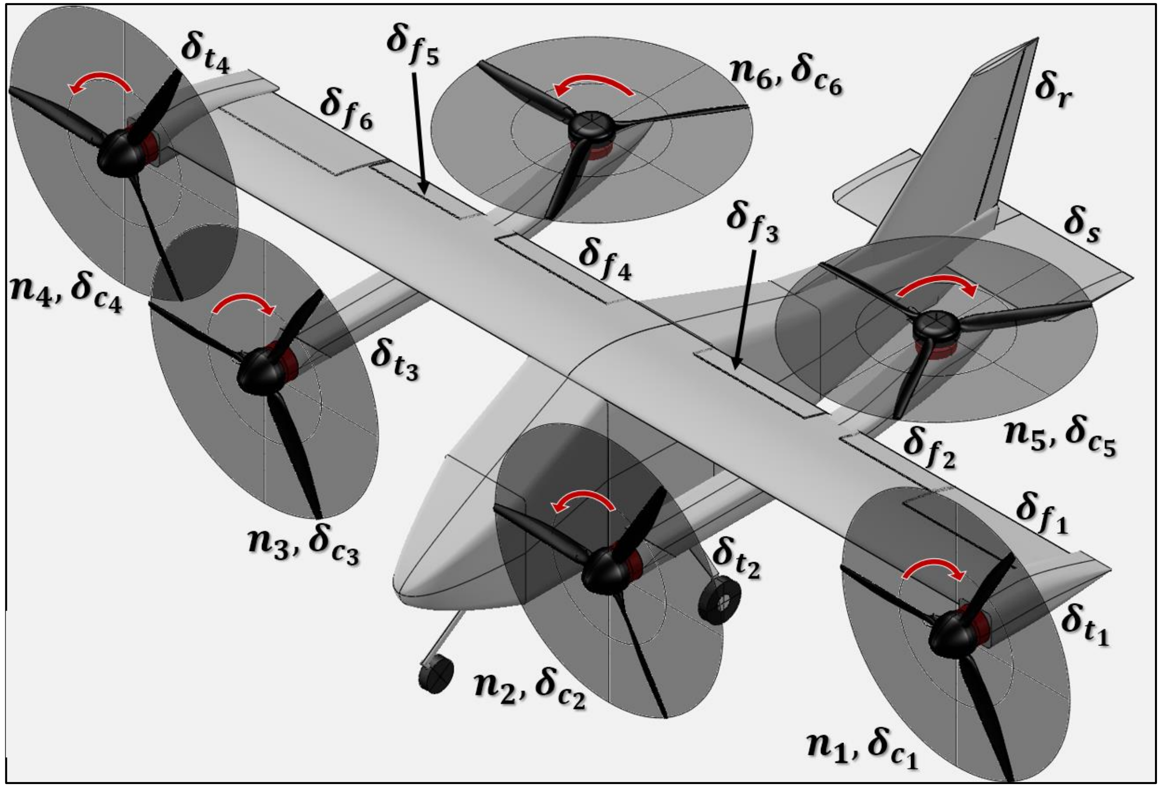

RAVEN control effector definitions.

1. German, B. J., Jha, A., Whiteside, S. K. S., and Welstead, J. R., "Overview of the Research Aircraft for eVTOL Enabling techNologies (RAVEN) Activity," *AIAA AVIATION Forum*, AIAA Paper 2023-3924, June 2023.

RAVEN-SWFT Vehicle

SWFT = **S**ubscale **W**ind-Tunnel and **F**light **T**est

- Wind-tunnel and flight-test research
- Similar in scale and utility to the NASA LA-8
- 28.6% scale version of 1000-lb vehicle
- 37 lbs, 5.7 ft wingspan, 19.5 in diam. proprotors

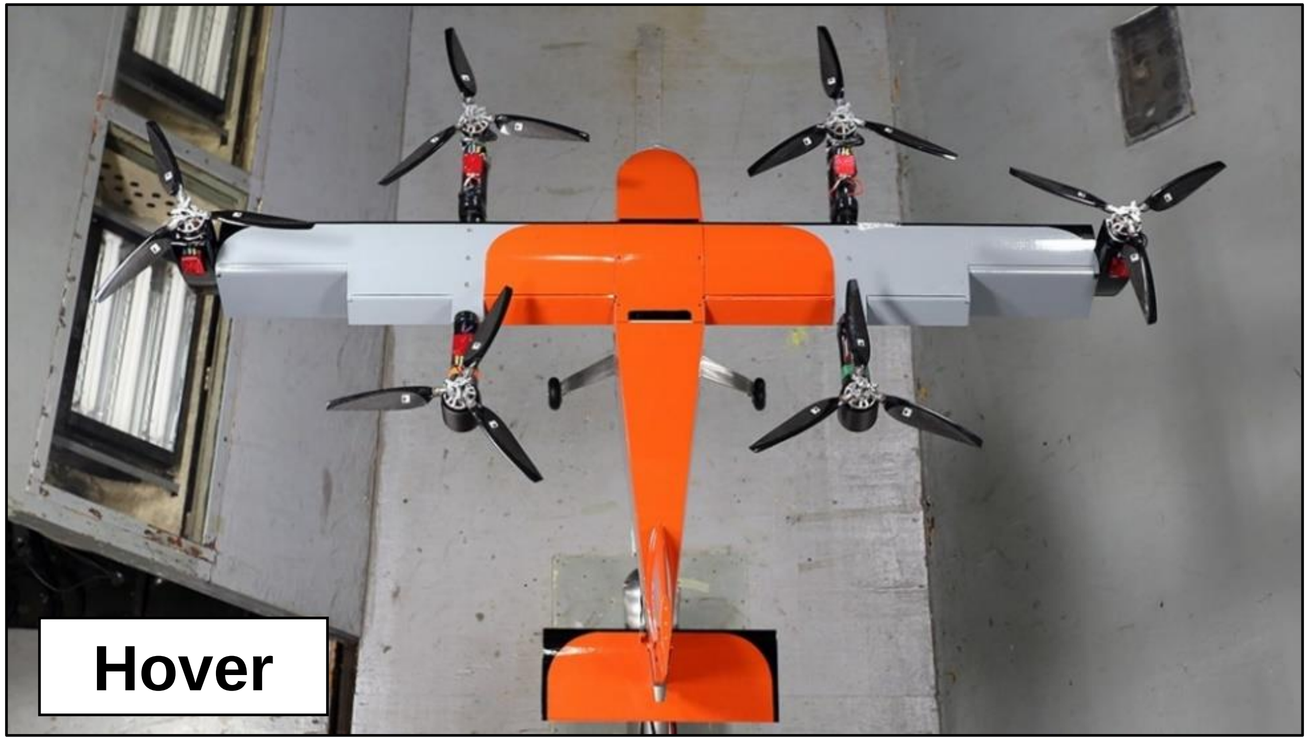

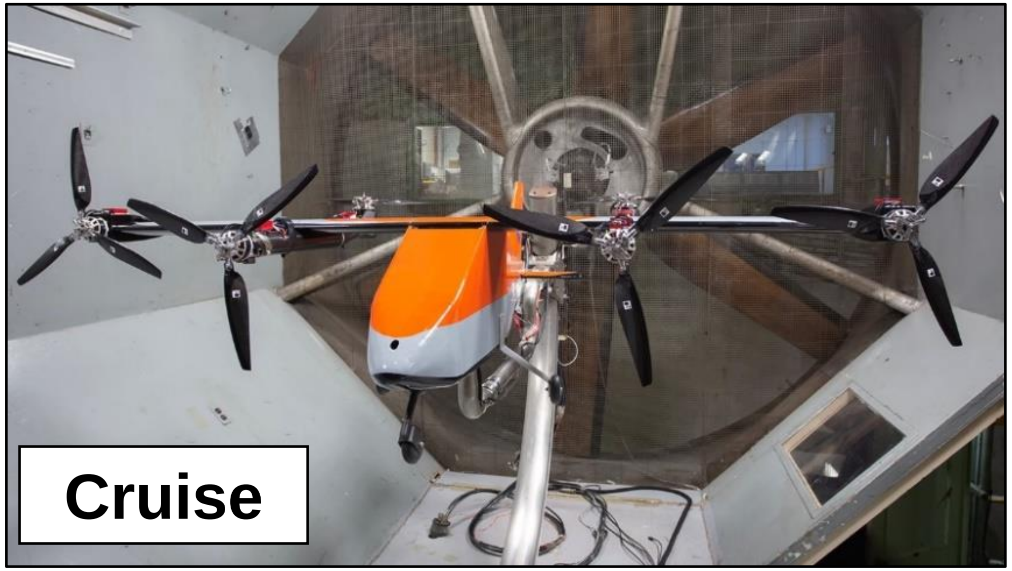

RAVEN-SWFT Wind-Tunnel Testing

Langley 12-Foot Low-Speed Tunnel

- Isolated proprotor test[1]
- **Static full-airframe test**
- Dynamic testing (in progress)

Static Full-Airframe Test Phases

- Gravitational tare modeling
- Trim envelope determination
- Powered-airframe characterization

Proprotor **Powered-airframe**

RAVEN-SWFT wind tunnel tests.

Benefits

- Flight simulation development
- Flight control system design
- Validation of prediction tools
- Data/models that can be published

1. Simmons, B. M., “Efficient Variable-Pitch Propeller Aerodynamic Model Development for Vectored-Thrust eVTOL Aircraft,” *AIAA AVIATION Forum*, AIAA Paper 2022-3817, June 2022.

Gravitational Tare Characterization

Test time reduced by nearly 50%

- Internal strain-gage balance measures:
  - Aero-propulsive forces and moments
  - Gravitational loads (i.e., aircraft weight)
- Gravitational loads must be removed
- Tare runs require additional test time
- eVTOL aircraft have large moving components
- Previous testing required many tare points
- New gravitational tare modeling approach
  - Application of DOE/RSM techniques
  - Powered-airframe test factors: $\alpha, \delta_{t_1}, \delta_{t_2}, \delta_{t_3}, \delta_{t_4}, \delta_{f_1}, \delta_{f_6}, \delta_s$
  - I-optimal response surface design (130 total points)
  - Model identified to predict gravitational loads
  - Obviates most required tare test time

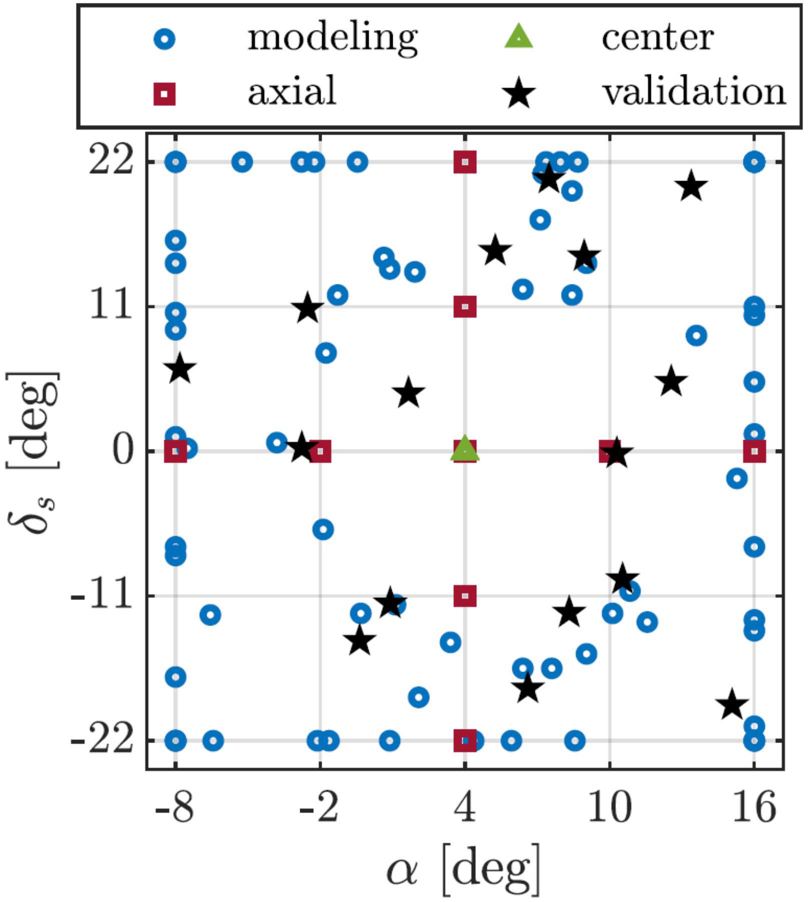

2D slice of the 8-factor tare experiment design.

Gravitational Tare Model Validation

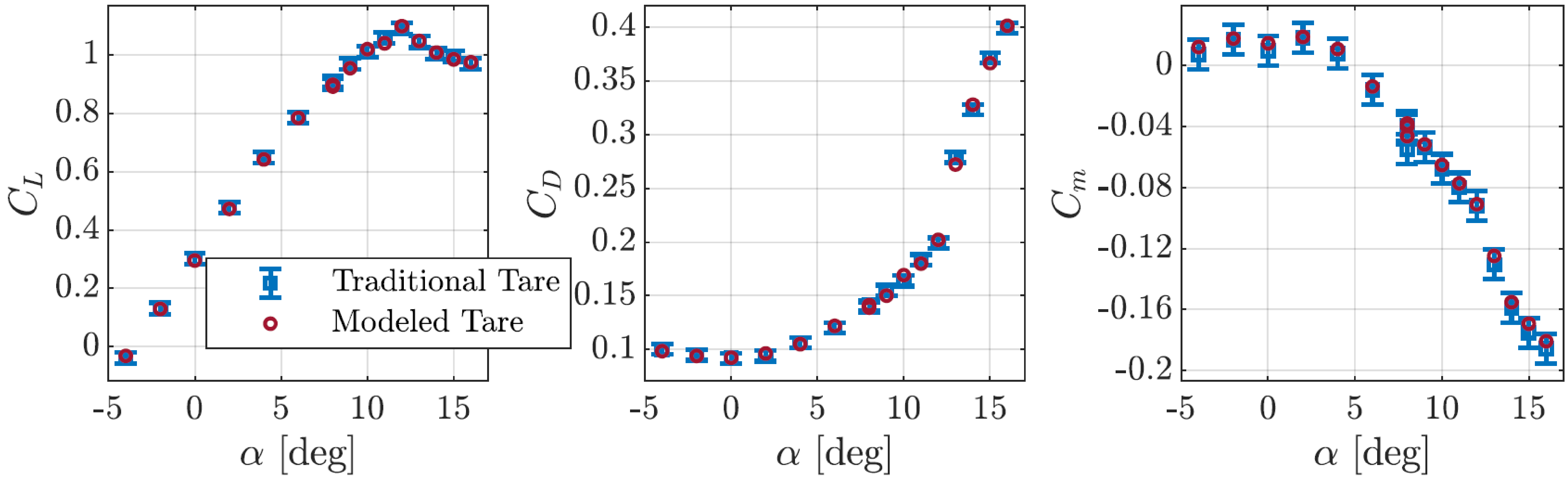

Isolated-airframe angle-of-attack sweep data collected at $\overline{q}$ = 3.5 psf using a traditional and modeled tare.

Transition Trim Envelope Determination

- Proper design space limits are important for transition characterization
- Specifying boundaries around the trim envelope is an effective approach
- The trim envelope was determined manually in previous wind-tunnel tests
- New trim approach using DOE/RSM
  - Efficient, accurate, and mostly automated
  - Testing with a reduced number of factors
  - Level, unaccelerated transition envelope
  - Results inform subsequent aero-propulsive characterization experiments

Trim Envelope Determination Strategy

- Progressive testing (increasing airspeed)
- Identify response surface equations
- Find control effector settings where:
  - Lift = Aircraft Weight = 37 lbf
  - Horizontal Thrust – Drag = 0 lbf
  - Pitching Moment = 0 ft-lbf
- Free control variables:
  - Front collective ($\delta_{c_{\mathrm{front}}}$)
  - Rear collective ($\delta_{c_{\mathrm{rear}}}$)
  - Nacelle tilt (δ_t)
- Fixed control variables (swept):
  - Proprotor rotational speed ($n_{\mathrm{front}} = n_{\mathrm{rear}}$)
  - Outboard flaperon angle ($\delta_{f_{\mathrm{out}}}$)
  - Inboard flaperon angle ($\delta_{f_{\mathrm{in}}}$)
- Root-finding algorithm finds trim solutions
- Near-real-time analysis capabilities

Trim Envelope Determination Experiment

- Eight dynamic pressure, $\bar{q}$, settings (low → high)
- Testing up to the highest attainable $\bar{q}$
- Seven test factors/explanatory variables:
  1. Front motor command/rotational speed (n_{front})
  2. Rear motor command/rotational speed (n_{rear})
  3. Front collective pitch angle ($\delta_{c_{\text{front}}}$)
  4. Rear collective pitch angle ($\delta_{c_{\text{rear}}}$)
  5. Nacelle tilt angle (δ_t)
  6. Outboard flaperon deflection angle ($\delta_{f_{\text{out}}}$)
  7. Inboard/midboard flaperon deflection angle ($\delta_{f_{\text{in}}}$)
- Frugal design strategy (56 points per $\bar{q}$ setting)
- I-optimal response surface design

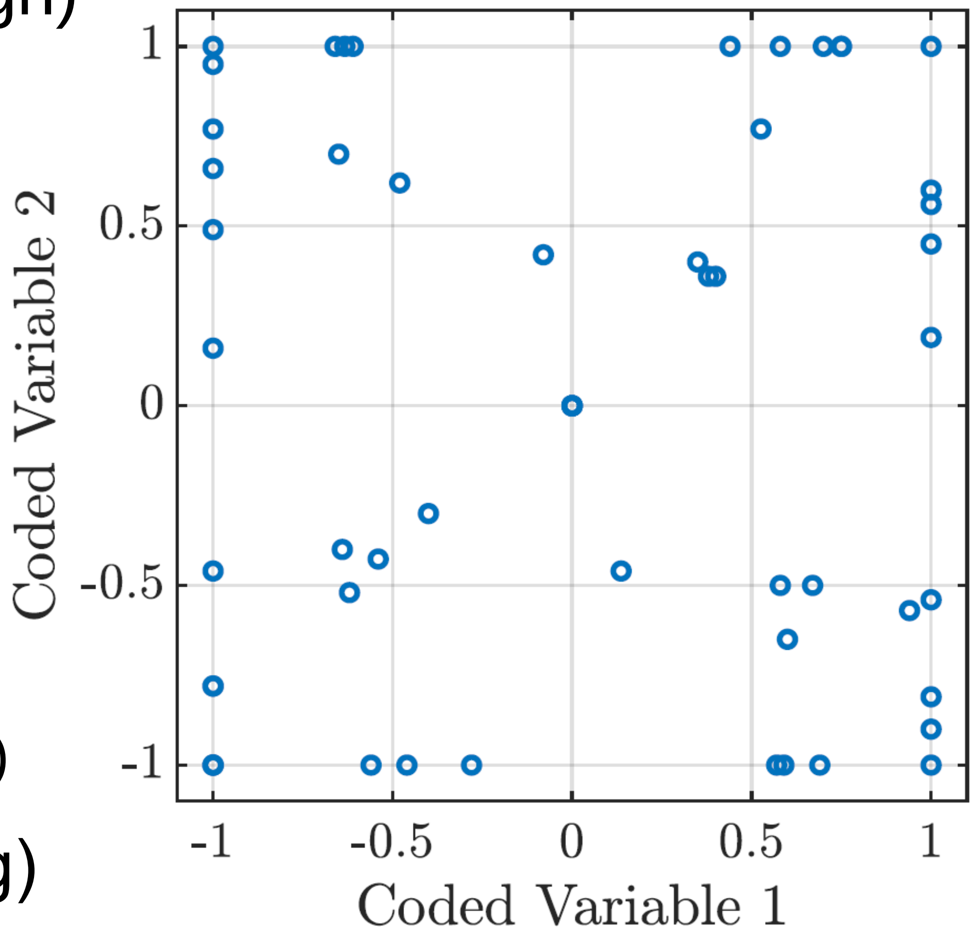

2D slice of the 7-factor trim experiment design in coded units.

Experimentally-Determined Trim Envelope

Proprotor rotational speed

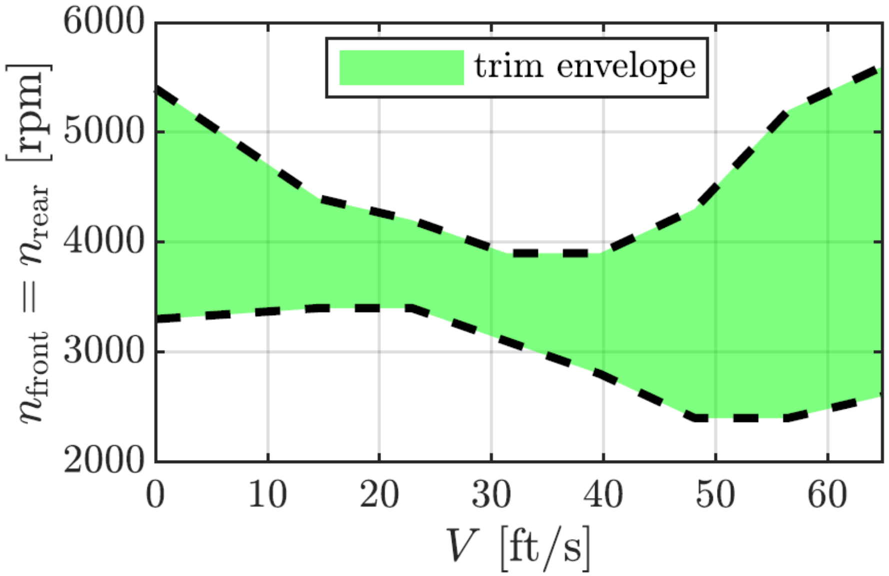

Nacelle Tilt Angle

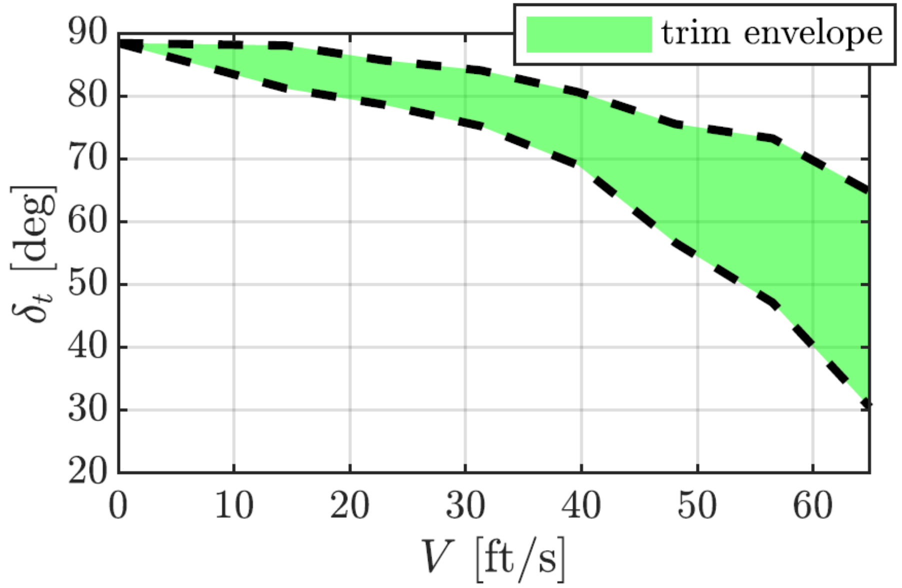

Front Collective Angle

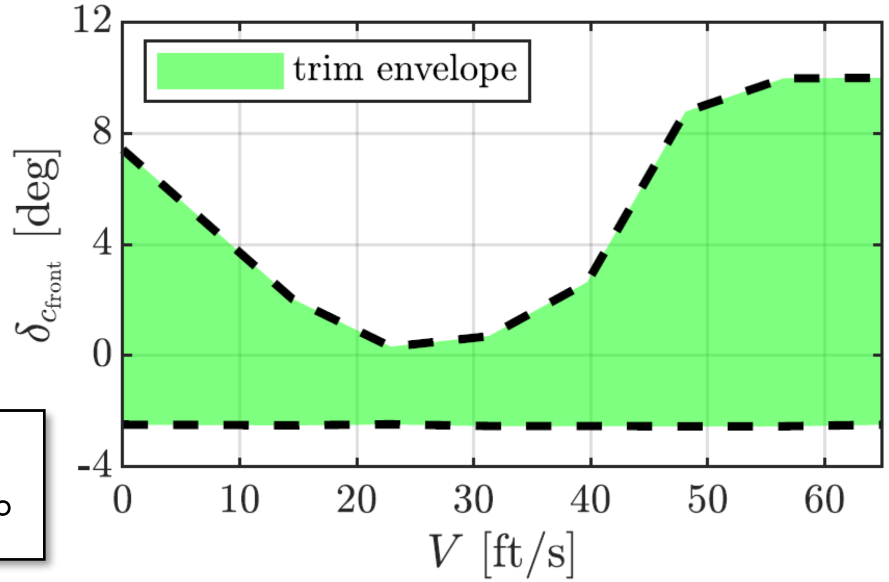

Rear Collective Angle

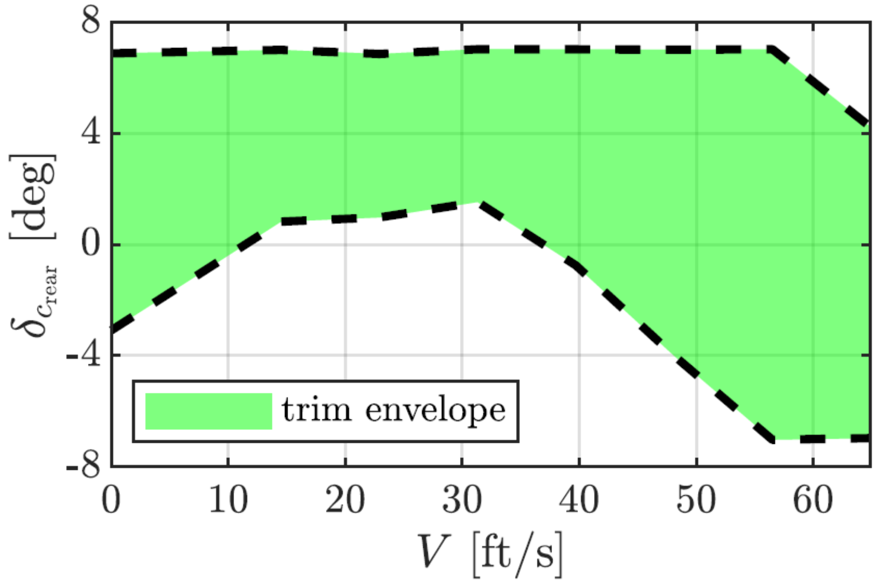

$\alpha = \beta = 0°$
$\delta_s = \delta_r = 0°$

Powered-Airframe Characterization

- Informed by the transition trim envelope determination results
- Powered-airframe testing from hover through mid-transition
- Eight dynamic pressure, $\bar{q}$, settings
- 26 independent test factors at each $\bar{q}$ setting
  - Angle of attack (α)
  - Angle of sideslip (β)
  - Motor speed commands ($\eta_{m_1}, \eta_{m_2}, \dots, \eta_{m_6}$)
  - Collective pitch angles ($\delta_{c_1}, \delta_{c_2}, \dots, \delta_{c_6}$)
  - Nacelle tilt angles ($\delta_{t_1}, \delta_{t_2}, \delta_{t_3}, \delta_{t_4}$)
  - Flaperon deflection angles ($\delta_{f_1}, \delta_{f_2}, \dots \delta_{f_6}$)
  - Stabilator deflection angle (δ_s)
  - Rudder deflection angle (δ_r)
- Nested I-optimal design[1] (984 points per $\bar{q}$)

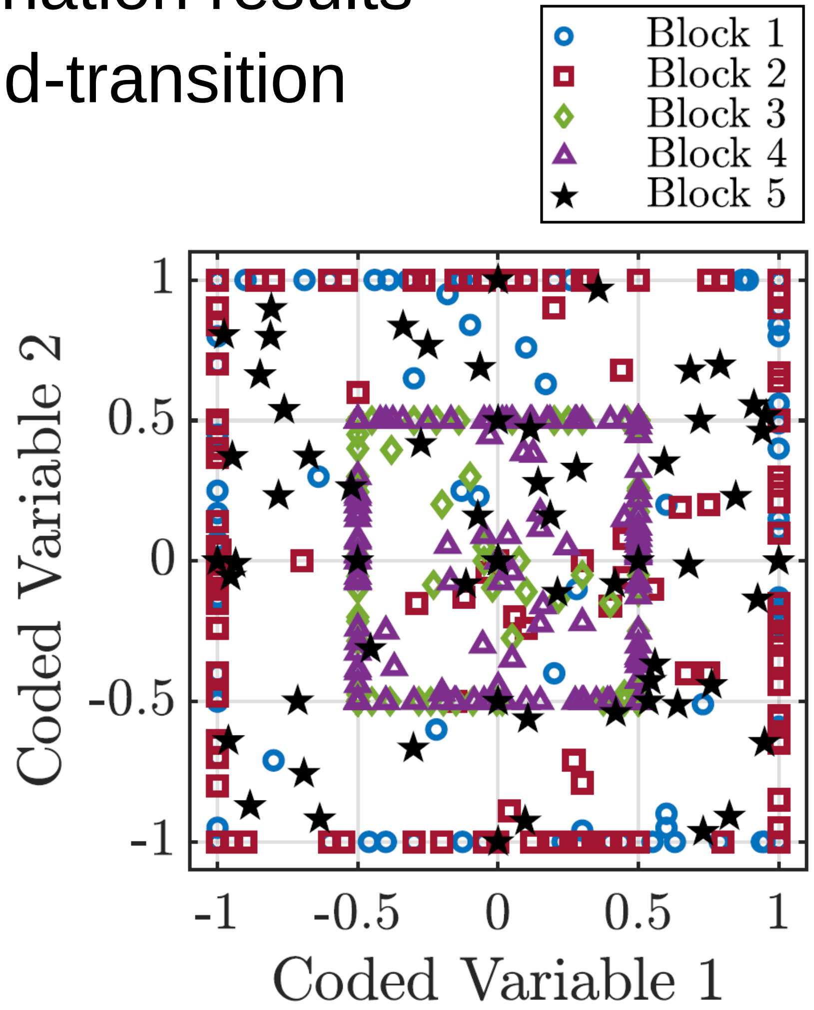

2D slice of the 26-factor experiment design in coded units.

1. Simmons, B. M., "Evaluation of Response Surface Experiment Designs for Distributed Propulsion Aircraft Aero-Propulsive Modeling," *AIAA SciTech Forum*, AIAA Paper 2023-2251, Jan. 2023.

RAVEN-SWFT Wind-Tunnel Testing Video

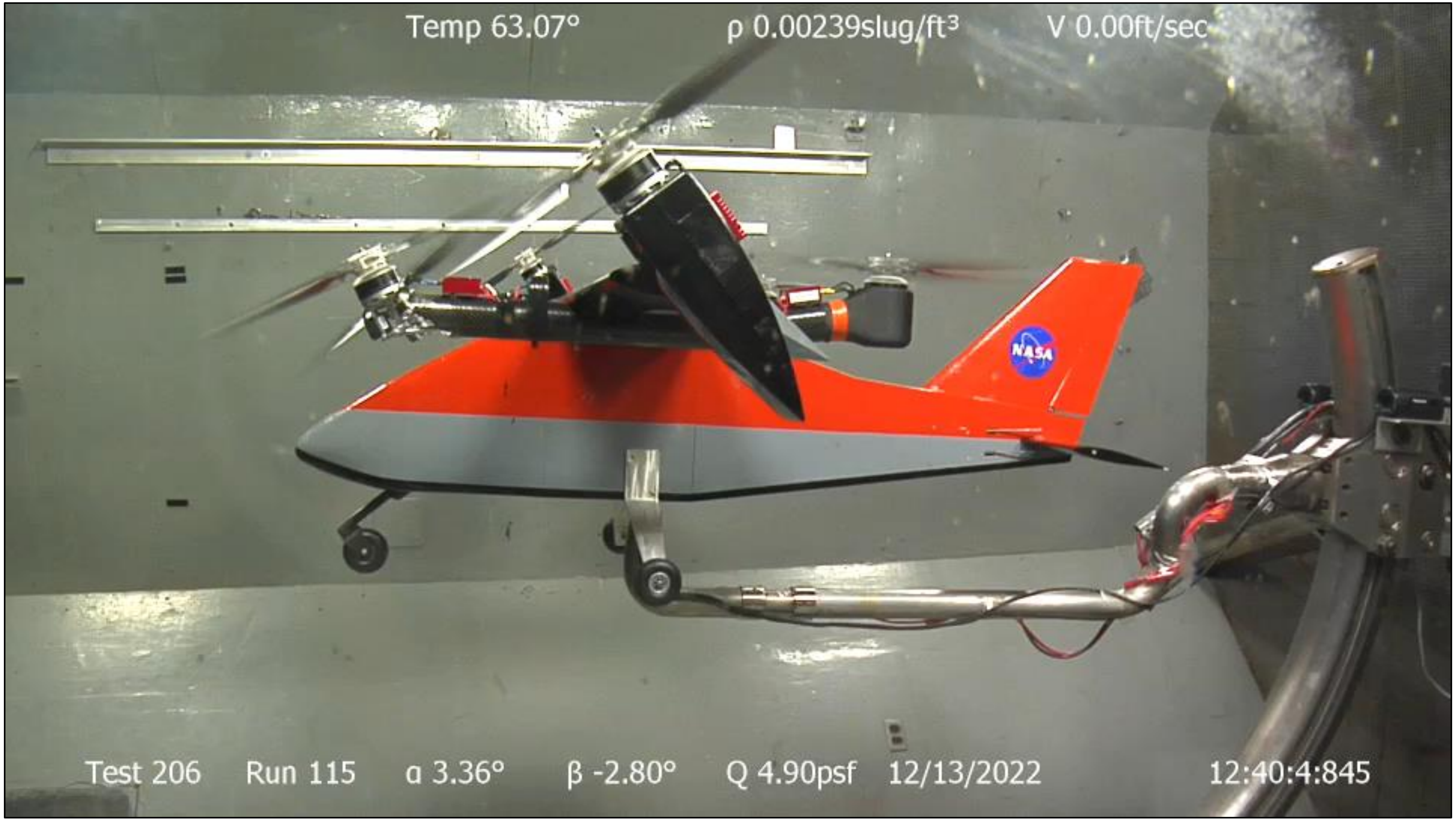

Static RAVEN-SWFT DOE/RSM wind-tunnel testing (x20 speed).

Powered-Airframe Model Identification

- Aero-propulsive modeling framework tailored to eVTOL aircraft[1]
- Flight condition variable: dynamic pressure $\bar{q}$ (or freestream velocity V)
- Explanatory variables:
  - Body-axis velocity components (v, w)
  - Proprotor rotational speeds $(n_1, n_2, \ldots, n_6)$
  - Control deflection angles $(\delta_{c_1}, \delta_{c_2}, \ldots, \delta_{c_6}, \delta_{t_1}, \delta_{t_2}, \delta_{t_3}, \delta_{t_4}, \delta_{f_1}, \delta_{f_2}, \ldots \delta_{f_6}, \delta_s, \delta_r)$

u effects are captured by models being developed at multiple $\bar{q}$ settings

- Response variables:
  - Dimensional body-axis aero-propulsive forces (X, Y, Z)
  - Dimensional body-axis aero-propulsive moments (L, M, N)
- Nonlinear response surface equations (RSEs) developed at each $\bar{q}$
  - Model structure determination: stepwise regression
  - Parameter estimation: ordinary least-squares regression
- Continuous transition model formed by interpolating between RSEs

$\bar{q}, v, w$
$n_1, n_2, \ldots, n_6$
$\delta_{c_1}, \delta_{c_2}, \ldots, \delta_{c_6}$
$\delta_{t_1}, \delta_{t_2}, \delta_{t_3}, \delta_{t_4}$
$\delta_{f_1}, \delta_{f_2}, \ldots \delta_{f_6}$
δ_s, δ_r

Aero-Propulsive Model

X, Y, Z, L, M, N

1. Simmons, B. M., and Murphy, P. C., "Aero-Propulsive Modeling for Tilt-Wing, Distributed Propulsion Aircraft Using Wind Tunnel Data," *Journal of Aircraft*, Vol. 59, No. 5, 2022, pp. 1162–1178.

Sample Local Modeling Results

- Z RSE at $\bar{q}$ = 2.75 psf compared to axial and center wind-tunnel data points
- RSE predictions show good agreement with measured data
- Data are within the 95% prediction interval (PI)
- Similar results observed for other response variables and $\bar{q}$ settings
- Sample residual diagnostics plots are shown in the paper

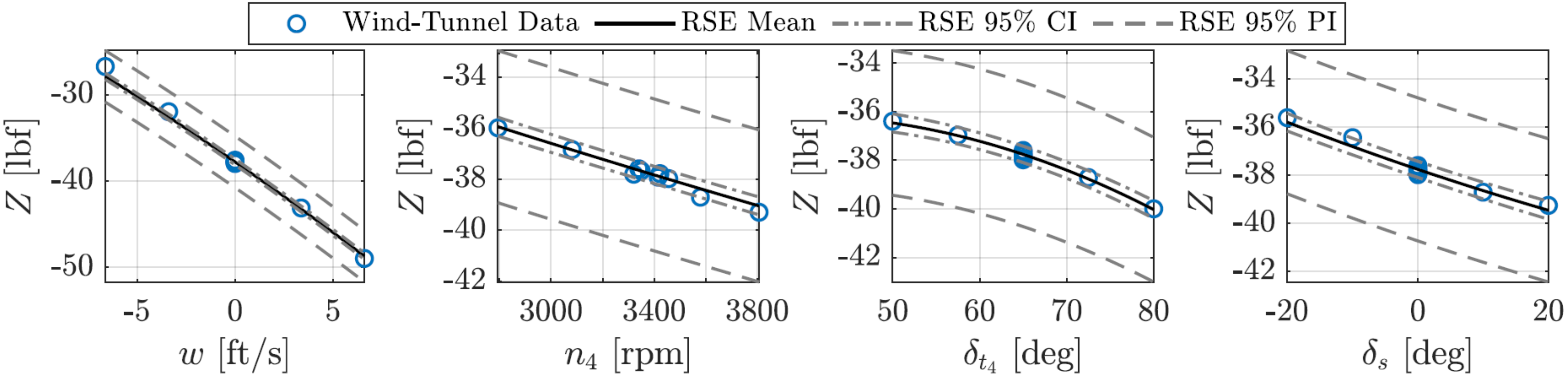

Model and wind-tunnel data comparison for explanatory variable sweeps ($\bar{q}$ = 2.75 psf).

Sample Global Modeling Results

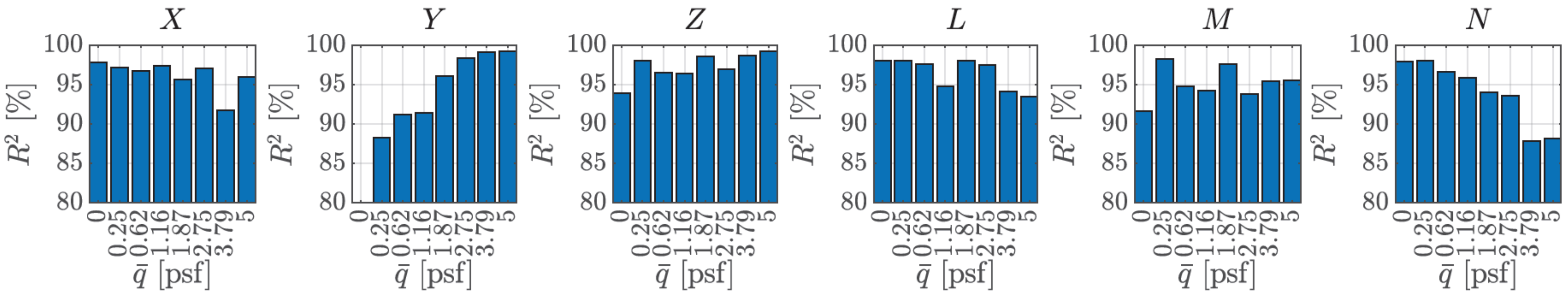

Coefficient of determination, R^2, for each local model.

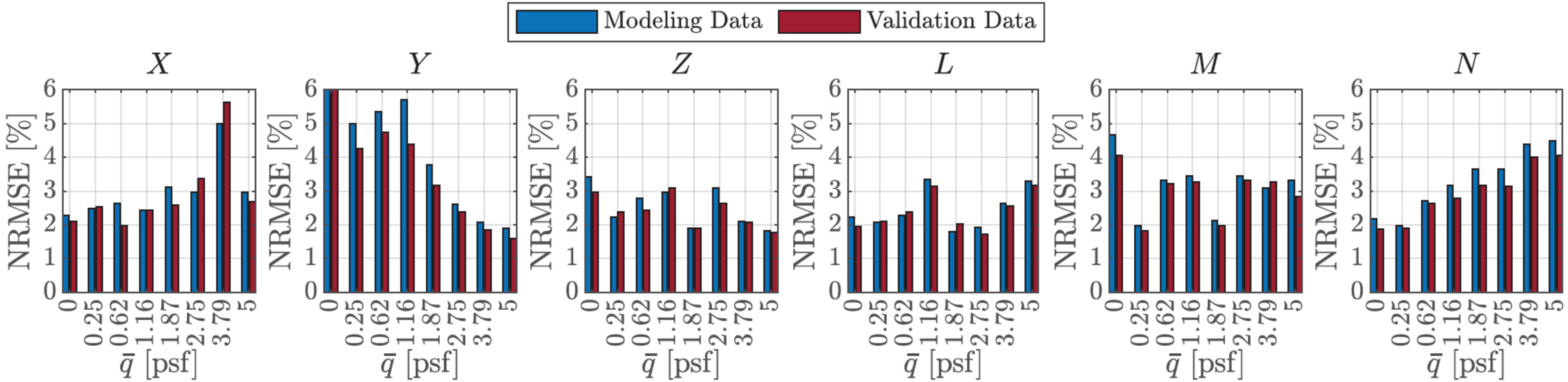

Modeling/validation normalized root-mean-square error (NRMSE) for each local model.

Concluding Remarks

- eVTOL aircraft present new aero-propulsive modeling challenges
- DOE/RSM techniques enable accurate characterization of complex aircraft
- Multiple advances in efficient eVTOL aircraft wind-tunnel testing
  - Gravitational tare experiment design and modeling approach
  - Experimental transition trim envelope determination strategy
  - Powered-airframe testing conducted using the nested I-optimal design
- Final aero-propulsive models have good predictive capability
- Techniques can be applied for many current and future eVTOL vehicles
- Active research is further refining eVTOL vehicle modeling techniques
- RAVEN project – strong emphasis on public release of data/technology

Look Ahead: NASA Langley FDRF

- Flight Dynamics Research Facility (FDRF)
- Scheduled to open in January 2025
- Replacing, combining, and expanding capabilities of the:
  - 20-Foot Vertical Spin Tunnel (VST)
  - 12-Foot Low-Speed Tunnel (LST)

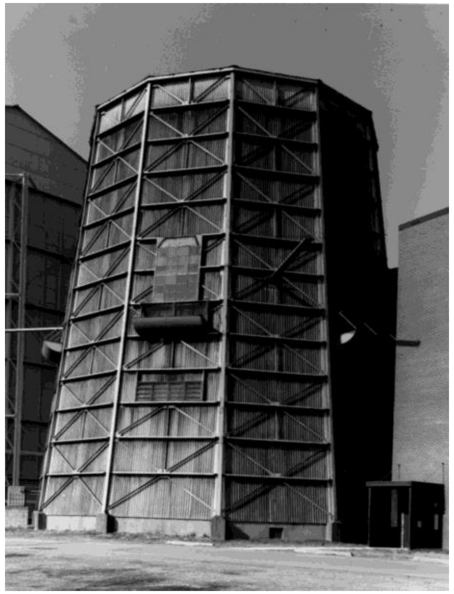

20-Foot VST

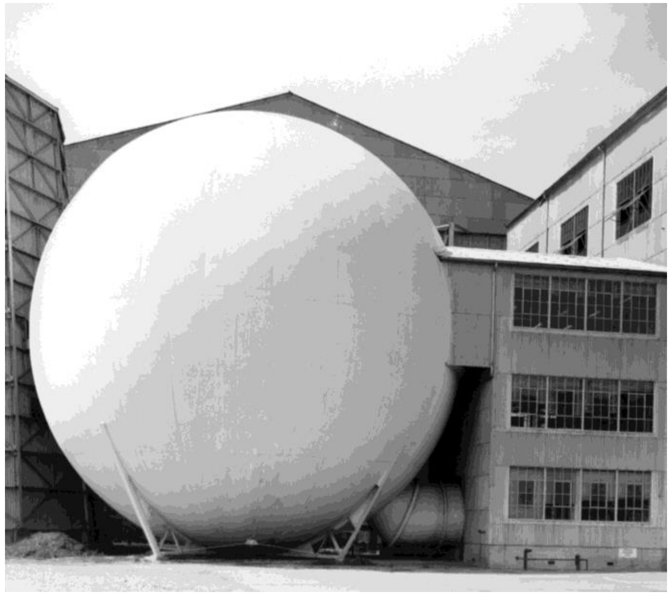

12-Foot LST

FDRF construction progress (Dec. 19, 2023)

Questions/Discussion – Thank you for attending.

Acknowledgments

- **Funding:** NASA Aeronautics Research Mission Directorate (ARMD) Transformational Tools and Technologies (TTT) Project
- **Wind-tunnel test support:** Wes O'Neal, Clinton Duncan, Rick Thorpe, Earl Harris, Lee Pollard, Sue Grafton
- **RAVEN-SWFT vehicle support:** Greg Howland, Matt Gray, Neil Coffey, Steve Geuther, Dave North
- **RAVEN project support:** Kasey Ackerman, Jake Cook, Steve Riddick, Siena Whiteside, Jason Welstead, Nat Blaesser
- **Gravitational tare modeling integration and validation support:** Stephen Farrell and Wes O'Neal

Related eVTOL Aircraft Modeling and RAVEN-SWFT References

1. Simmons, B. M. and Murphy, P. C., "Aero-Propulsive Modeling for Tilt-Wing, Distributed Propulsion Aircraft Using Wind Tunnel Data," *Journal of Aircraft*, Vol. 59, No. 5, 2022, pp. 1162–1178.
2. Simmons, B. M., Geuther, S. C., and Ahuja, V., "Validation of a Mid-Fidelity Approach for Aircraft Stability and Control Characterization," *AIAA AVIATION Forum*, AIAA Paper 2023-4076, June 2023.
3. Simmons, B. M., "Evaluation of Response Surface Experiment Designs for Distributed Propulsion Aircraft Aero-Propulsive Modeling," *AIAA SciTech Forum*, AIAA Paper 2023-2251, Jan. 2023.
4. Simmons, B. M., "Efficient Variable-Pitch Propeller Aerodynamic Model Development for Vectored-Thrust eVTOL Aircraft," *AIAA AVIATION Forum*, AIAA Paper 2022-3817, June 2022.
5. Busan, R. C., Murphy, P. C., Hatke, D. B., and Simmons, B. M., "Wind Tunnel Testing Techniques for a Tandem Tilt-Wing, Distributed Electric Propulsion VTOL Aircraft," *AIAA SciTech Forum*, AIAA Paper 2021-1189, Jan. 2021.

Backup Slides

RAVEN-SWFT Modeling and Controls

Flight Testing

Validation

Wind-Tunnel Testing

Validation

Computational Predictions

RAVEN-SWFT Flight Dynamics Model

Flight Control System Development

Research Advancement and Toolchain Validation Enabled by RAVEN-SWFT

Gravitational Tare Model Validation

RSE = Response Surface Equation
PI = Prediction Interval

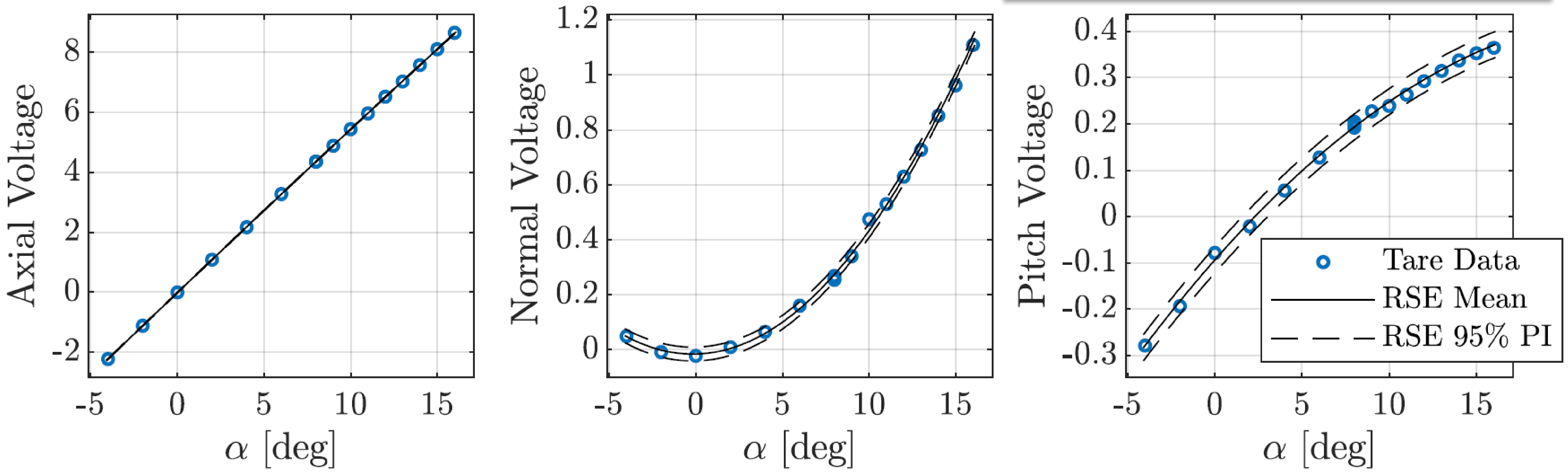

Gravitational tare voltage data and model predictions for an isolated-airframe angle-of-attack sweep data at $\overline{q}$ = 3.5 psf.

Powered-Airframe Experiment Design

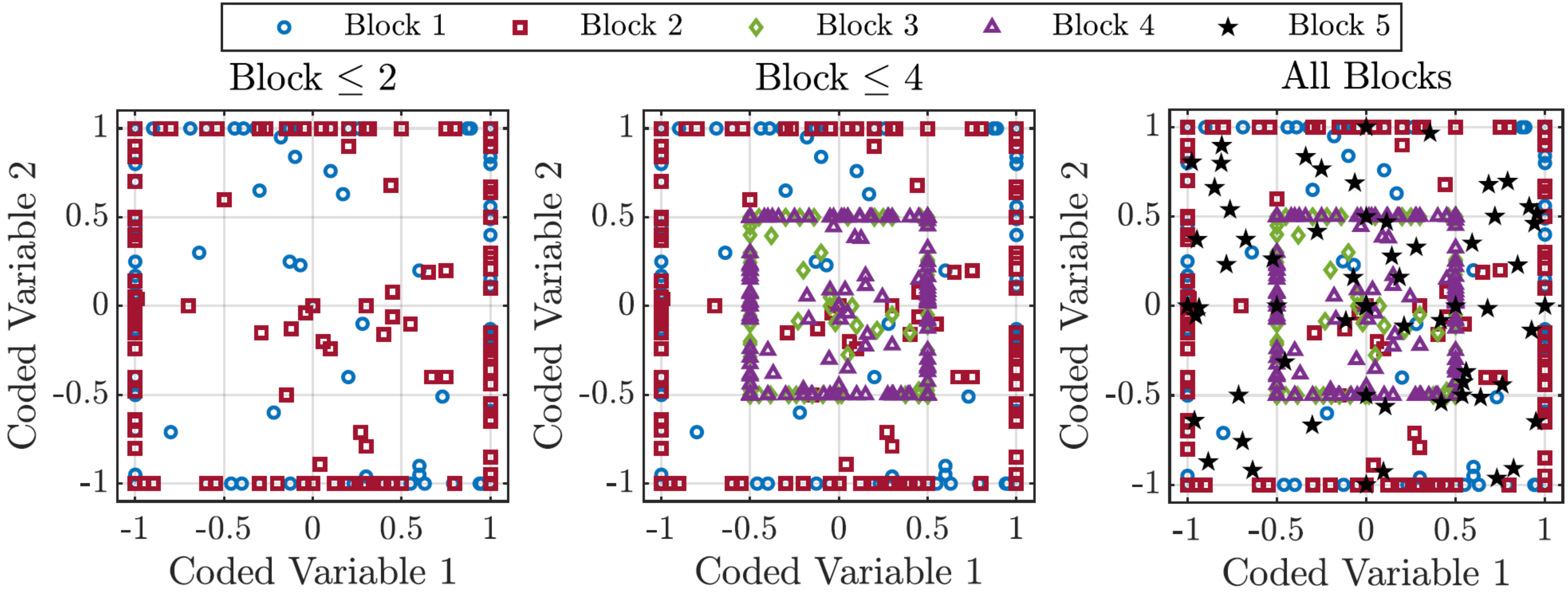

Fig. 7 Sequential two-dimensional slices of the 26-factor powered-airframe characterization experiment design.

Powered-Airframe Experiment Design

Table 8 Powered-airframe experiment design summary

Block Number	Design Type	Design Model	Model Points	Center Points	Axial Points	Validation Points	Total Points	Cumulative Points
1	I-optimal	quadratic (1/2)	202	3	0	0	205	205
2	I-optimal	quadratic (2/2)	203	3	0	0	206	411
3	nested I-optimal	quadratic (1/2)	203	3	0	0	206	617
4	nested I-optimal	quadratic (2/2)	202	3	0	0	205	822
5	validation	N/A	0	6	104	52	162	984

Powered-Airframe Experiment Design

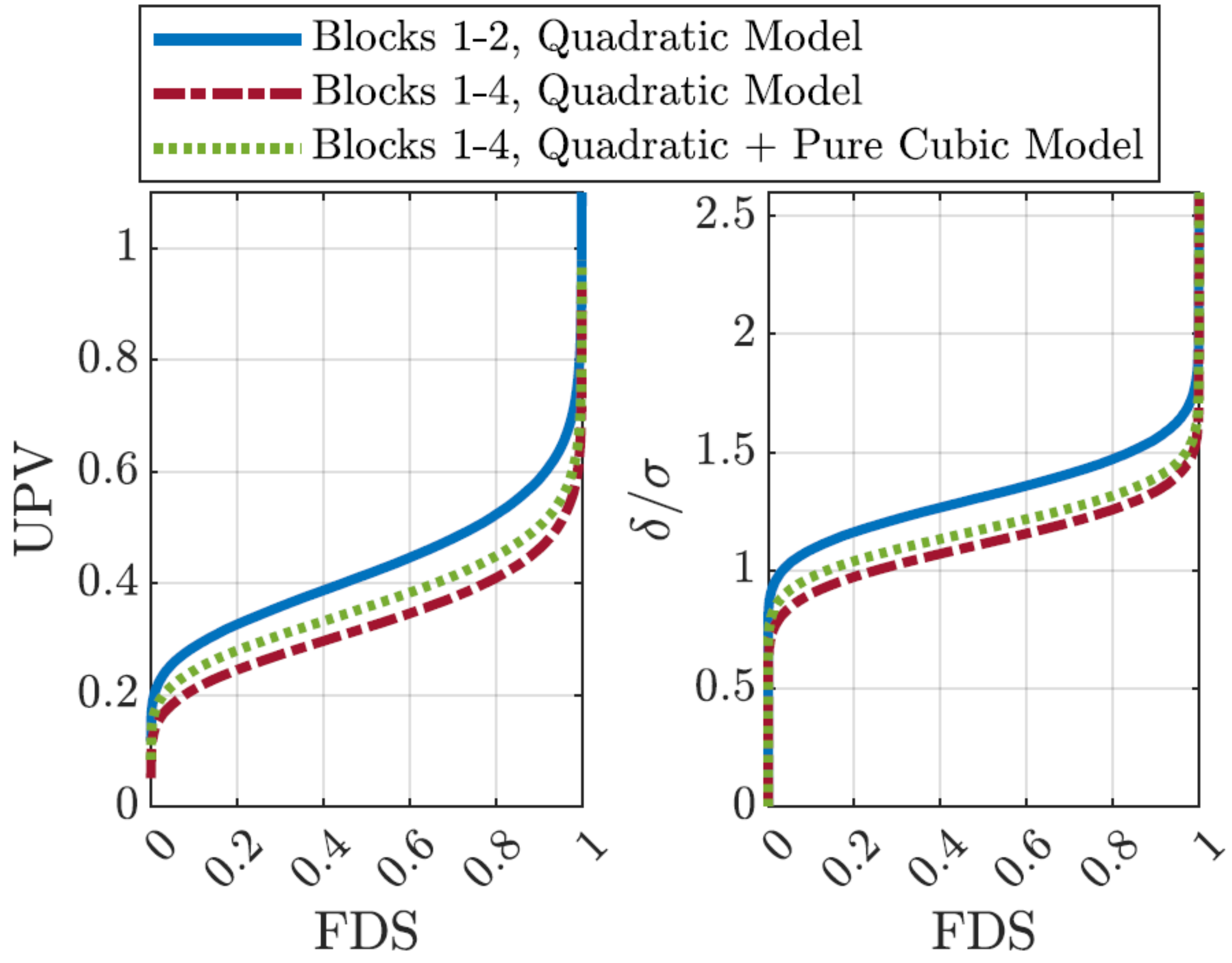

Fig. 8 Prediction variance plots for the 26-factor powered-airframe experiment design.

Table 9 Prediction variance threshold FDS values for the powered-airframe experiment design

Blocks	Evaluation Model	FDS with $\delta/\sigma \leq 1.5$	FDS with $\delta/\sigma \leq 2$
1-2	Quadratic	0.837	0.999
1-4	Quadratic	0.986	1.000
1-4	Quadratic + Pure Cubic	0.970	1.000

Powered-Airframe Modeling Results

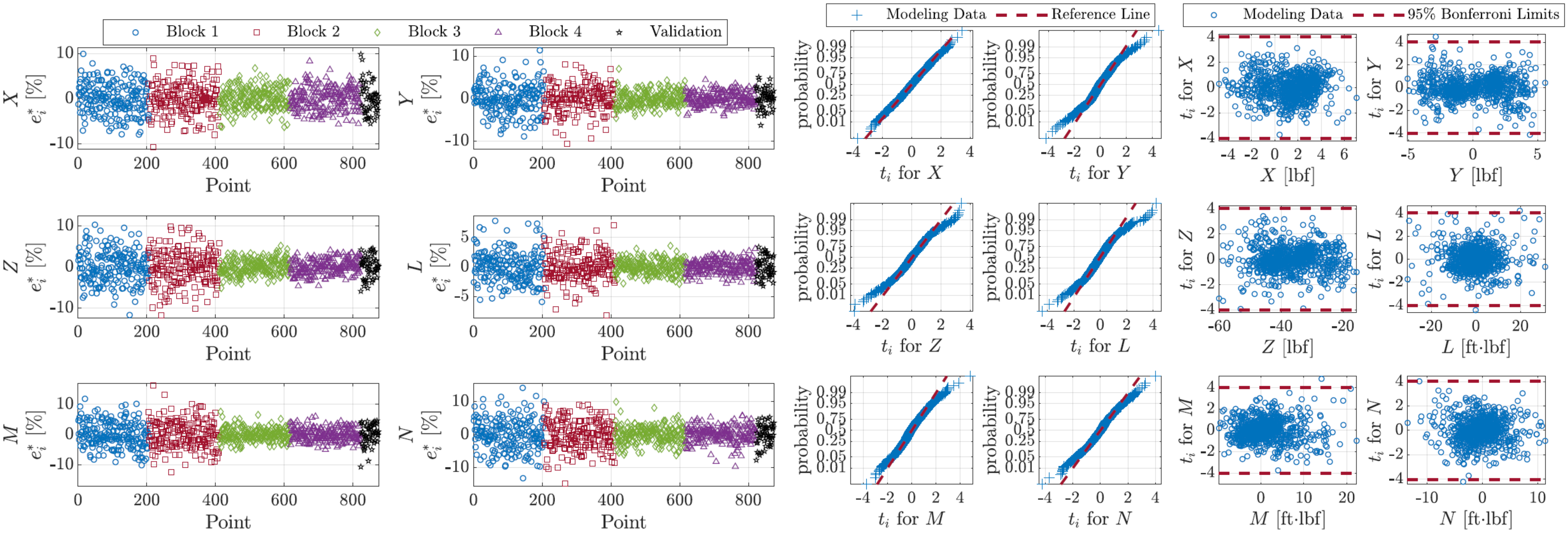

(a) Residual history

(b) Normal probability plot

(c) Residuals against predicted response

Fig. 9 Residual diagnostics for the powered-airframe model at $\bar{q}$ = 2.75 psf.

Powered-Airframe Modeling Results

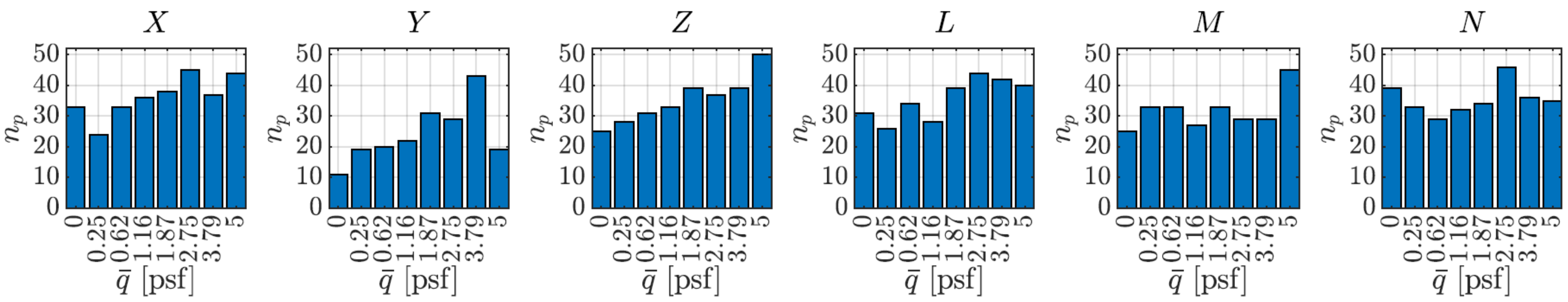

Fig. 12 Number of model parameters, n_p, identified for each local model response.

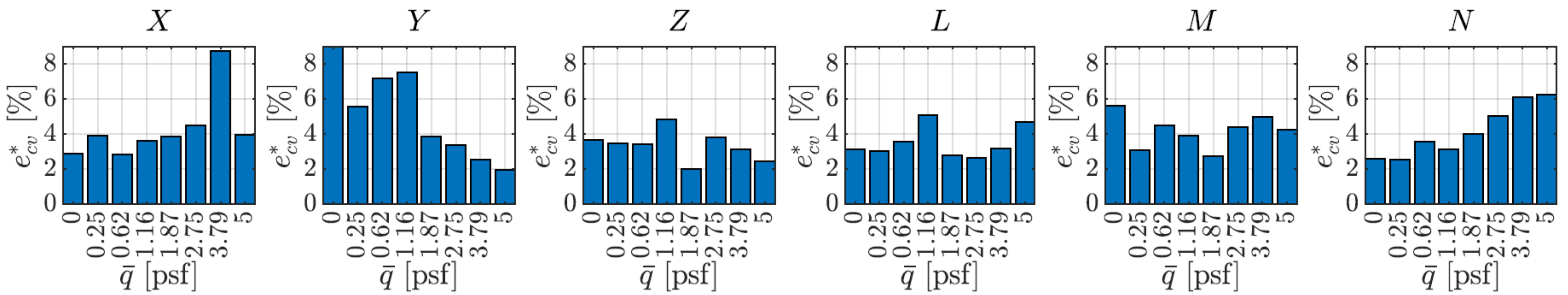

Fig. 14 Binomial analysis of residuals prediction error metric, e_{cv}^*, for each local model response.